EPJ Web of Conferences **21**, 08001 (2012)
DOI: 10.1051/epjconf/20122108001

Neutron induced fission of ^{234}U

F.-J. Hambsch[1], A. Al-Adili[1,2], S. Oberstedt[1], S. Pomp[2]

[1]EC-JRC-Institute for Reference Materials and Measurements, Retieseweg 111, B-2440 Geel, Belgium
[2]Uppsala University, Uppsala, Sweden

Abstract. The fission fragment properties of ^{234}U(n,f) were investigated as a function of incident neutron energy from 0.2 MeV up to 5 MeV. The fission fragment mass, angular distribution and kinetic energy were measured with a double Frisch-grid ionization chamber using both analogue and digital data acquisition techniques. The reaction ^{234}U(n,f) is relevant, since it involves the same compound nucleus as formed after neutron evaporation from highly excited ^{236}U*, the so-called second-chance fission of ^{235}U. Experimental data on fission fragment properties like fission fragment mass and total kinetic energy (TKE) as a function of incident neutron energy are rather scarce for this reaction. For the theoretical modelling of the reaction cross sections for Uranium isotopes this information is a crucial input parameter. In addition, ^{234}U is also an important isotope in the Thorium-based fuel cycle. The strong anisotropy of the angular distribution around the vibrational resonance at E_n = 0.77 MeV could be confirmed using the full angular range. Fluctuations in the fragment TKE have been observed in the threshold region around the strong vibrational resonance at E_n = 0.77 MeV. The present results are in contradiction with corresponding literature values. Changes in the mass yield around the vibrational resonance and at E_n = 5 MeV relative to E_n = 2 MeV show a different signature. The drop in mean TKE around 2.5 to 3 MeV points to pair breaking as also observed in ^{235,238}U(n,f). The measured two-dimensional mass yield and TKE distribution have been described in terms of fission modes. The yield of the standard 1 (S1) mode shows fluctuations in the threshold of the fission cross section due to the influence of the resonance and levels off at about 20% yield for higher incident neutron energies. The S2 mode shows the respective opposite behaviour. The mean TKE of both modes decreases with E_n. The decrease in mean TKE overrules the increase in S1 yield, so the mean TKE is dropping as a function of E_n above 2.5 MeV.

1 Introduction

The neutron induced fission of ^{234}U is interesting in several respects. First of all it is a threshold reaction with a (or even several) strong vibrational resonances at the threshold of the fission cross section. As it seems to be the case also for other isotopes around these vibrational resonances in the fission cross section threshold the properties of the fission fragments are changing as it has been found in the work of Goverdovskii [1]. However, in a similar experiment on ^{238}U(n,f) the previously

observed fluctuations in literature of the fission fragment properties in the vibrational resonances in the fission cross section threshold could not be verified [2].

Furthermore this isotope is the daughter of the ^{235}U(n,f) reaction after second chance fission, setting in from about 6 MeV incident neutron energy. Hence the investigation of the reaction ^{234}U can lead to important input parameters in the theoretical modelling of the reaction cross section as well as prompt neutron emission probabilities of ^{235}U(n,f). Last but not least ^{234}U is also an important isotope in the Th-U fuel cycle, for which a recent IAEA-Coordinated Research Project (CRP) resulted in new reaction cross section evaluations [3]. Further improvements of the available database and especially the knowledge of the fission fragment mass and total kinetic energy (TKE) distributions will help to improve on the prompt neutron emission properties. These data are input data for model calculations e.g. with the Point by Point (PbP) model [4]. For ^{234}U(n,f) not many experimental results in terms of fission fragment properties are available in the literature.

Finally, the angular anisotropy of the fission fragments showed a very strong change around the vibrational resonance at about 0.8 MeV [5-7]. Whether this has a consequence on other fission fragment properties like mass and kinetic energy needs to be verified.

2 Experimental set-up

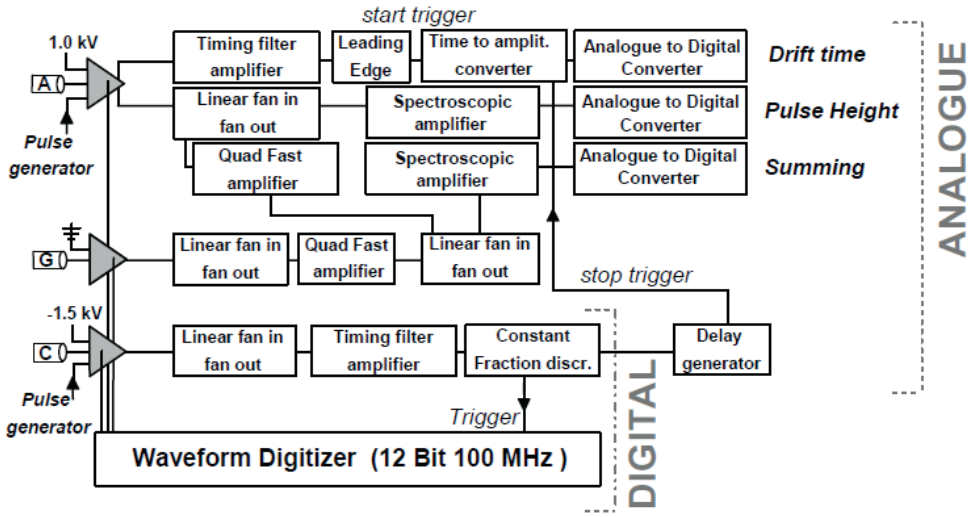

Fig. 1. Schematical set-up of the electronic scheme.

The experiments are performed at the 7 MV Van de Graaff accelerator at the Institute for Reference Materials and Measurements (IRMM) in Geel, Belgium. The fission fragments are detected by means of a Twin Frisch Grid Ionization Chamber (TFGIC) with two anodes, two grids and a common cathode. As counting gas P10 (90% Argon, 10% Methane) is used in continuous flow. The Uranium sample, with a thickness of 92 μg/cm^2, was produced through vacuum evaporation on gold-coated polyimide foil. The neutron production is done using three nuclear reactions, TiT(p,n), TiD(d,n), and ^{7}LiF(p,n). The TiT(p,n) and TiD(d,n) reactions provide higher count rates due to the thickness of the target sample, but with significantly higher energy uncertainty at lower neutron energies. Therefore the ^{7}LiF(p,n) reaction with a thinner ^{7}Li-sample is used in the low neutron energy region below 1 MeV.

The Uranium sample is located in the centre of the cathode. Energies and angles of both fragments are measured using the double E method, conservation of energy and momentum is assumed to calculate FF masses. The absolute calibration for the energy uses the known literature

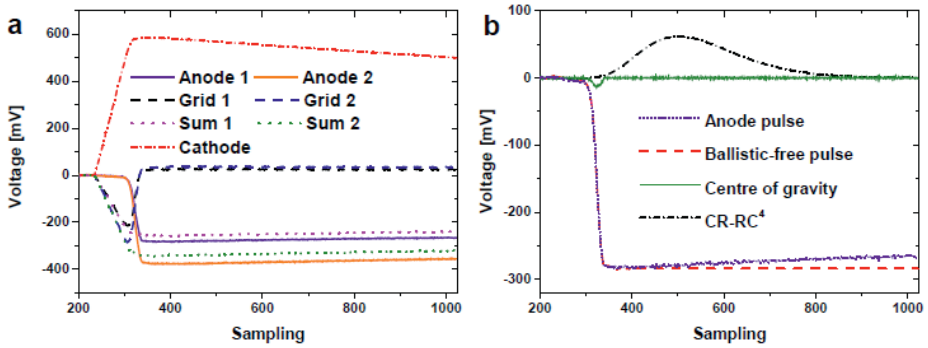

Fig. 2. Wave-forms after baseline correction and sum signal production. b: Wave-form differentiation (full line) and ballistic-deficit correction followed by the CR - RC^4 alter using t = 0.5 μs in shaping time. One channel corresponds to 10 ns.

data on thermal induced fission of ^{235}U (45 μg/cm^2). The recommended total kinetic energy TKE = 170.5 +/- 0.5 MeV and the position of the mean heavy-mass peak at A_H = 139.6 amu are used for the absolute energy calibration .

3 Data analysis

Five signals were extracted from the TFGIC (two anodes, two grids and one cathode signal). Data acquisition was done in parallel, using both analogue and digital acquisition systems. A schematical view of the electronics needed for each chamber side is presented in Fig. 1.

The signals are directly fed into a charge-sensitive preamplifier. The preamplifiers are put close to the chamber (short cables) in order to store the total collected charge with minimal signal-noise contribution.

Once charges start to drift in the grid-cathode space, the chamber voltage drops corresponding to an equal reduction of charge storage across the capacitance in the pre-amplifier. The output voltage V_{out} is proportional to the induced charge provided that the decay time of the preamplifier is long compared with the pulse rise-time. Typical FF rise-time in the TFGIC are about 0.1 - 0.5 μs compared with the decay time of the preamplifier of 100 μs.

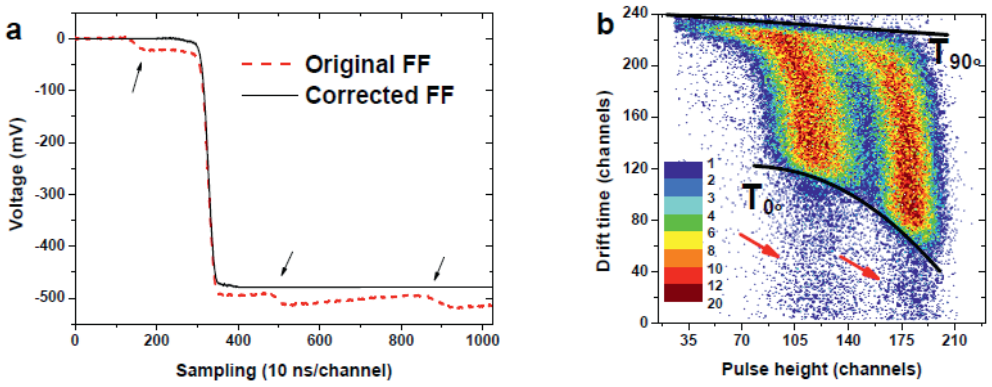

Fig. 3. a: One event from ^{234}U(n, f), with three α-particle pile-up events before correction (dashed line) and after the correction (full line). b: Drift-time versus pulse-height distribution. False triggering from early α-particle pile-up is observed as time-uncorrelated events (indicated by the arrows).

Although for both analogue and digital systems data acquisition has been performed. The final data analysis was mainly done for the digital system, due to its superiority over the analogue data.

Figure 2a shows the typical traces of the different electrodes of the ionisation chamber. Figure 2b shows the different analysis steps (ballistic deficit correction, centre of gravity determination and pulse height determination via the CR-RC^4 filter). In Figure 3a a trace of the anode is shown, which also shows several α-particle pile-up events on top of the anode trace, due to the high α–activity of the ^{234}U target (about 150 kBq). Via digital signal processing those α-pile up events could be eliminated from the pulse and the pulse height determined, hence the event could be used in the final analysis. In an analogue case such events would be removed by a pile-up rejection system and would be lost in the final analysis. Due to the high α-activity nearly every event was affected by pile-up. The right part of Figure 3 shows the effect of α-pile-up in the drift time. Here the trigger position is compromised due to early α-pile-up and those are then observed as time-uncorrelated events in the spectrum (indicated by the arrows). A large part of these events can actually still be removed by sophisticated filtering techniques especially looking for early α–pile up events [8].

Table 1 summarises the studied energies, neutron producing reaction, respective fission cross section and counting statistics of the present experiment. The emphasis of the investigated neutron energies was put on the strong vibrational resonance region (around 0.8 MeV incident neutron energy).

Table 1. Measured neutron energies, reaction targets used, fission cross section and counting statistics.

E_n [MeV]	Reaction target thickness [$\mu g/cm^2$]	σ [barns] [4]	Counts [$\times 10^3$]
0.2 ± 0.07	^{7}LiF (p, n) 830	0.06	12
0.35 ± 0.06	^{7}LiF (p, n) 830	0.20	38
0.5 ± 0.05 (± 0.04)	^{7}LiF (p, n) 830, (619)	0.51	143
0.64 ± 0.03	^{7}LiF (p, n) 596	0.84	366
0.77 ± 0.03	^{7}LiF (p, n) 596	1.20	153
0.835 ± 0.03	^{7}LiF (p, n) 619	1.22	80
0.9 ± 0.03	^{7}LiF (p, n) 596, (619)	1.14	172
1.0 ± 0.1	TiT (p, n) 1936	1.10	128
1.5 ± 0.09 (± 0.1)	TiT (p, n) 1930, 1936, 2130	1.37	350
2.0 ± 0.08 (± 0.09)	TiT (p, n) 1930, 2130	1.52	967
2.5 ± 0.07	TiT (p, n) 1930, 1936	1.51	672
3.0 ± 0.06	TiT (p, n) 1936	1.10	272
4.0 ± 0.3	TiD (d, n) 1902	1.38	53
5.0 ± 0.18	TiD (d, n) 1902	1.33	130
^{235}U (n_{th}, f)	TiT (p, n) 1930, 2130	>500	2914

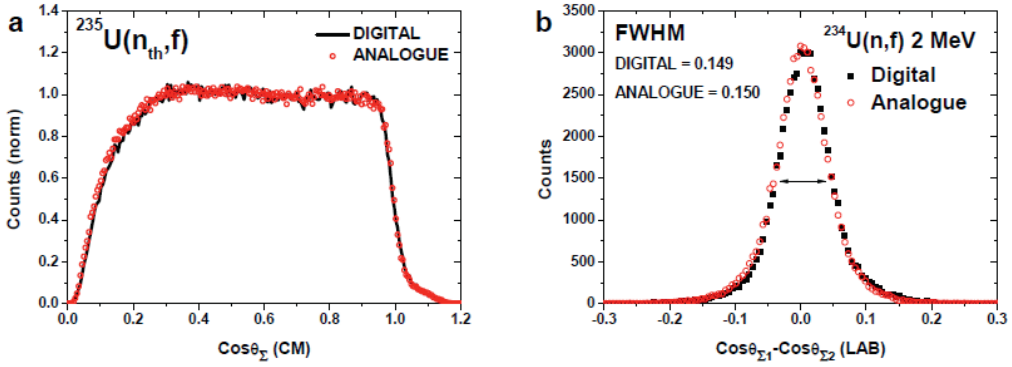

Fig. 4. a) Cosine distributions in the CM system for the isotropic reaction ^{235}U(n$_{th}$, f). b) The difference between the cos θ distribution, from the two TFGIC sides. The angular resolution is about 0.15 at FWHM for both digital and analogue acquisition.

Around this resonance also the angular distribution of the fission fragments is drastically changing as will be seen in the next chapter. The angular distribution is calculated using the angle dependent grid signal of the ionisation chamber. As calibration the ^{235}U(n,f) reaction at thermal incident neutron energy has been used, as for this energy the angular distribution is isotropic. Figure 4 shows the cosine distributions in the centre-of-mass (CM) system for ^{235}U(n$_{th}$,f) (Figure 4a), the achieved angular resolution comparing the analogue and digital analysis (Figure 4b). In Figure 5 a, b the cosine distributions are shown for two incident neutron energies of ^{234}U(n,f) at 2 MeV and 0.5 MeV, demonstrating the strong positive and negative anisotropy for this nucleus.

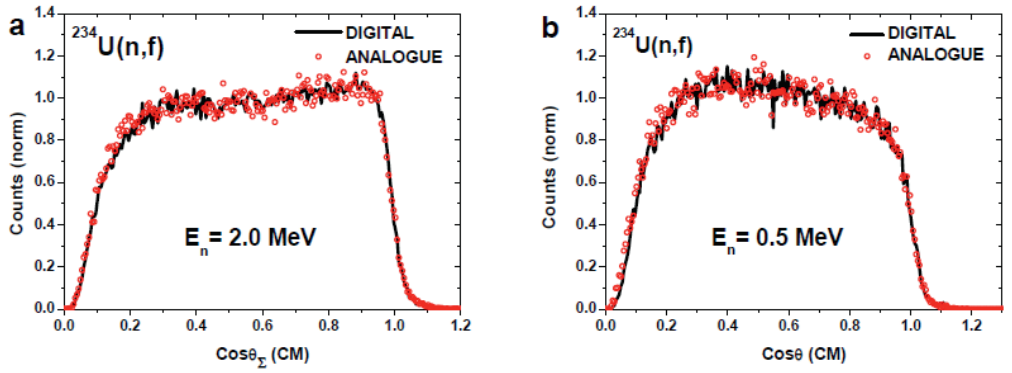

Fig. 5. Cosine distribution for the anisotropic ^{234}U(n, f) at 2 MeV (a) and 0.5 MeV (b).

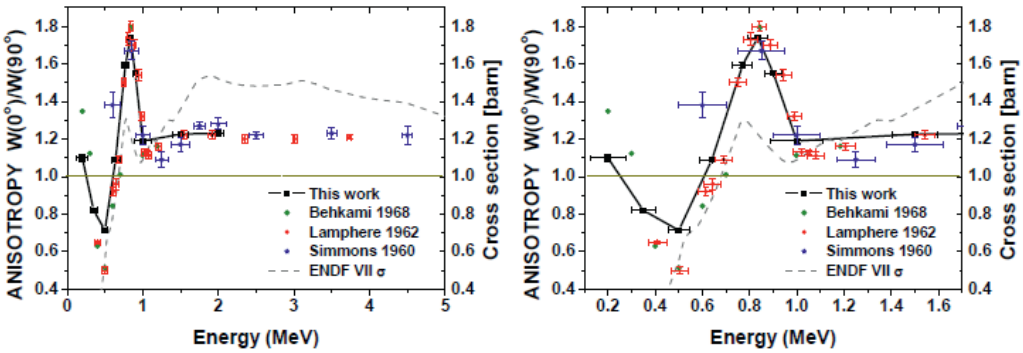

Fig. 6. Strong fluctuations in angular anisotropy as a function of incident neutron energy.

4 Results and discussion

The angular anisotropy is calculated using the ratio of the cosine distributions for ^{234}U(n,f) at a given incident neutron energy and the isotropic distribution of ^{235}U(n_{th},f). Then this ratio is fitted with the two first even Legendre polynomials. The resulting anisotropy is shown in Figure 6. The left part shows the full incident neutron energy range covered, the right part focuses the region of the vibrational resonances around 0.8 MeV. The present results are compared to literature data (Refs. [5-7]) taken in the 1960s. Very good agreement is observed especially with Refs. [5, 7], except around 0.5 MeV where our anisotropy is not as low as given in the literature. The advantage of the present experiment compared to the literature data is the fact that with the ionisation chamber we cover a nearly 2x2π angular range, whereas in former times a few selected angles were chosen for the measurements. It is also remarkable that the peak in the anisotropy is not coinciding with the resonance peak as shown with the dashed line in Figure 6, which depicts the fission cross section.

This has been observed in other compound systems with vibrational resonances in the threshold of the fission cross section (e.g. ^{238}U(n,f) [2]). In addition to the angular distribution also the mass and total kinetic energy distributions for ^{234}U(n,f) have been calculated using energy and momentum conservation. Results for ^{234}U(n,f) at 2 MeV (used as a reference to which all other incident neutron energies have been compared to) and the ^{235}U(n_{th},f) absolute reference are shown in Figure 7. Clear deviations to the ^{235}U data are observed for the TKE(A) distribution as a function of fission fragment mass. There are also differences in the mass distribution but not as prominent as for the TKE

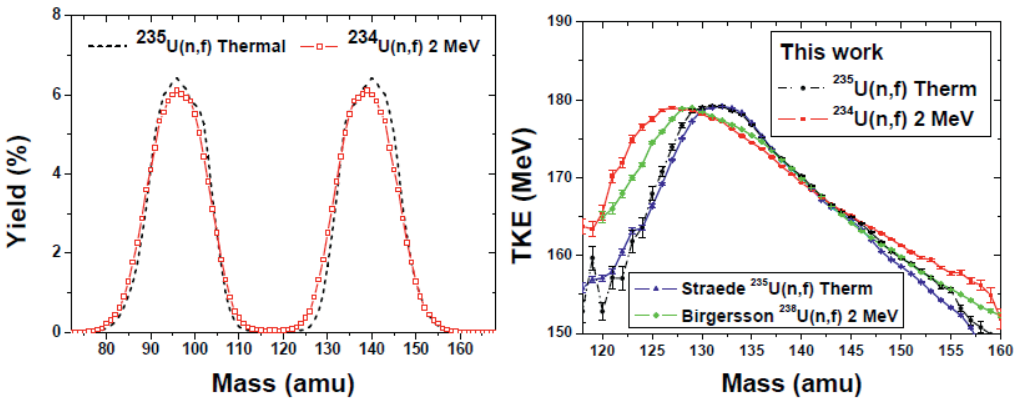

Fig. 7. Mass (left part) and total kinetic energy (TKE, right part) distributions for 2 MeV incident neutron energy on ^{234}U and the thermal reference ^{235}U.

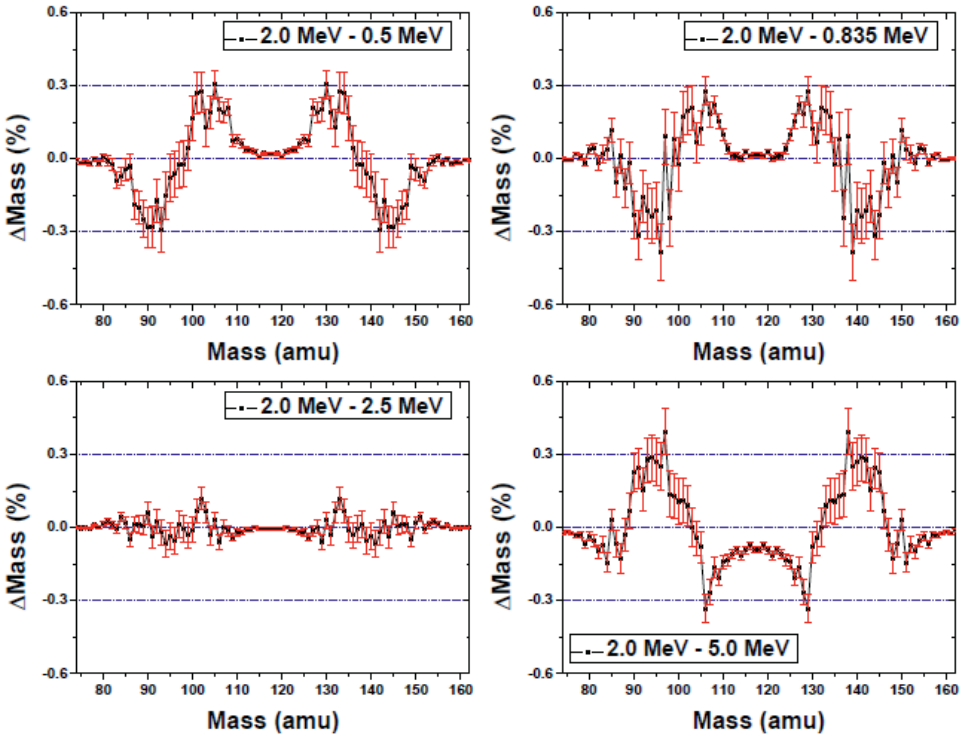

Fig. 8. Changes in the mass distributions for the given energy in the insert relative to the one at 2 MeV incident neutron energy.

distribution. In the right part of Figure 7 also results from literature [2, 9] have been included. The present dta for $^{235}U(n_{th},f)$ (black dots) compare very well with the ones of Ref. [9]. The data of Ref. [2] are just added for comparison and are different to the present $^{234}U(n,f)$ and $^{235}U(n_{th},f)$ data as the compound system in Ref. [2] is ^{239}U.

We also looked at changes in the mass yield distribution going from one incident neutron energy to the other. In Figure 8 as an example the difference of the mass yield at 2 MeV to the mass yield at 0.5 MeV, 0.835 MeV, 2.5 MeV and 5 MeV is given. A clear difference of the mass yield below the threshold is observed manifesting in a higher yield for mass ranges A = 85 to 100 (complementary mass A = 135 to 150) and a reduction in the mass yield for the mass range A = 100 to 115 (complementary mass A = 120 to 135) compared to 2 MeV. In contrast at the higher energies of 5 MeV the mass yield is reduced for masses A around 90 to 105 (complementary mass A = 130 to 145). An increase in symmetry for this energy is also evident as expected.

Changes in the TKE as a function of mass are also observed. Figure 9 shows the present results. At the peak of the anisotropy at E_n = 0.835 MeV the difference in TKE(A) between 2 MeV and 0.835 MeV is more or less constant in favour of the TKE(A) at 2 MeV incident neutron energy being higher over the majority of mass yield from about A = 126 to 155. In the minimum of the anisotropy at 0.5 MeV incident neutron energy the tendency of the difference in TKE(A) to 2 MeV is changed and it shows a increase in the positive bias at 2 MeV towards heavier masses. The whole picture changes at 5 MeV incident neutron energy. Here we see a clear trend of decreasing difference with increasing fragment mass A. Comparing this behaviour to the neighbouring isotopes $^{235}U(n,f)$ [9] and $^{238}U(n,f)$ [2, 10] one observes similarities (e.g. in $^{238}U(n,f)$) but also differences (e.g. in $^{235}U(n,f)$).

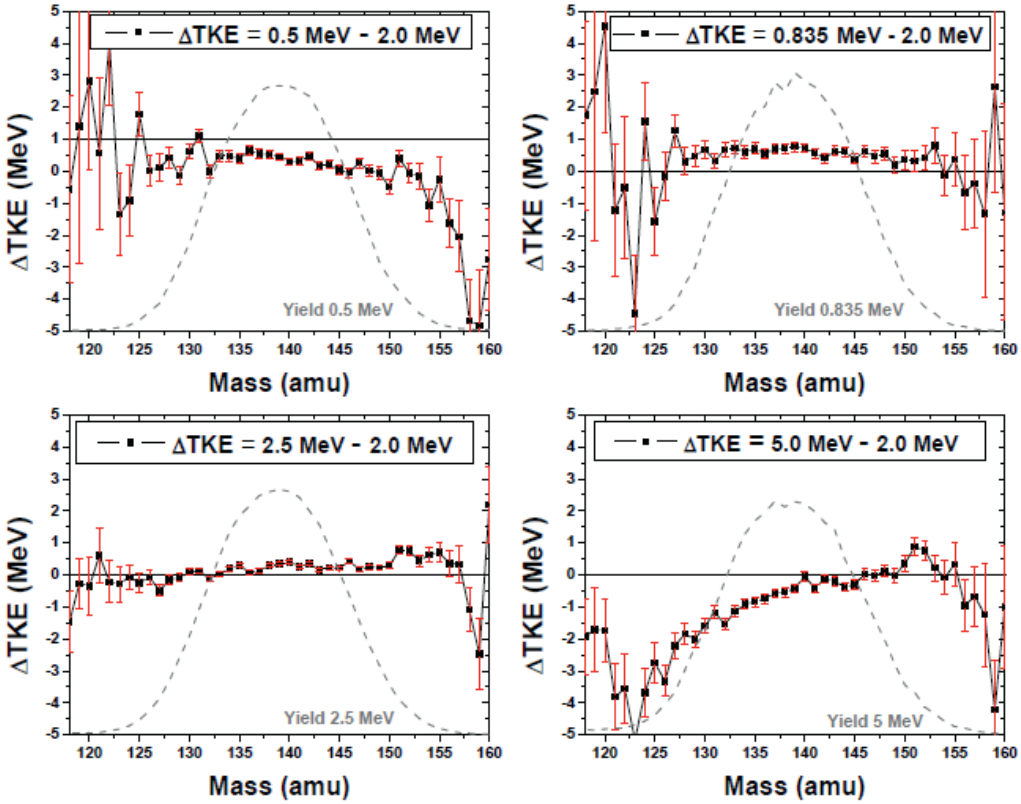

Fig. 9. Changes in the TKE distributions for the given energy in the insert relative to the one at 2 MeV incident neutron energy. The mass yield is indicated by the dashed line.

For the latter the behaviour of the TKE(A) distribution is quite different showing some peaking around the masses A = 130-132. Concerning the changes in the mass distribution in Ref. [9] no information is given. For ^{238}U(n,f) [2, 10] the changes below the threshold are not significant due to the very low cross section and hence limited statistics at the vibrational resonance energy of about 1.2 MeV. At 5.5 MeV the mass yield difference shows a reduction in yield in the inner wing of the mass distribution over a rather narrow mass region of only about 10 mass units (A = 100 – 110 amu) (see Figure 9 of Ref. [10]).

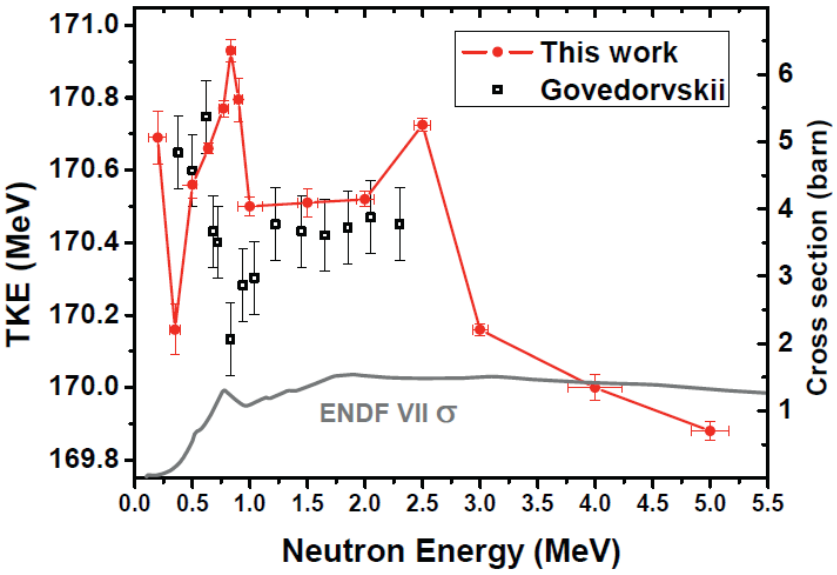

Fig. 10. Variation of the average TKE as a function of incident neutron energy. The present data (full circles) are compared to the data of Ref. [1] (open squares). The full line indicates the fission cross section.

Figure 10 shows the mean TKE as a function of incident neutron energy compared to Ref. [1]. The absolute mean TKE values are close to the ones of ^{235}U(n,f) [9] except around the vibreational resonance region. The behaviour as a function of incident neutron energy is also quite similar to ^{235}U(n,f). However around the vibrational resonance we observe the opposite behaviour as given in Ref. [1]. The present values for the mean TKE are higher in the resonance compared to Ref. [1], where a dip in mean TKE is observed. Also towards the minimum in the anisotropy at 0.5 MeV we see a dip in the mean TKE whereas Ref. [1] observed higher values. A possible explanation could be the fact that in Ref. [1] surface barrier detectors have been used. Corrections for energy loss in the detector and the coverage of the full angular cone in 2x2π are more critical with those detectors. As the anisotropy is strongly changing around the vibrational resonance, coverage of the full solid angle is crucial. Unfortunately in Ref. [1] not much detail is given on this aspect.

Figure 11 shows the analysis of the mass and TKE distributions in terms of the multi-modal random-neck rupture model of Brosa et al. [11]. The two-dimensional mass versus TKE distribution (left part of Fig. 11) is fitted using Gaussian distributions for the mass yield distribution and skewed Gaussian distributions for the TKE distribution. The fitting program has been developed in the ROOT language [12]. Figure 11 shows the positions of the distributions in two dimensions in the left part and the contribution of the so-called standard 1 and 2 (S1 and S2) and super-long (SL) fission modes in the mass distribution of ^{234}U(n,f) at an incident neutron energy of 2 MeV in the right part. The fit is performed at all the investigated neutron energies. The behaviour of the different fit parameters is exemplified in Figure 12. Figure 12 shows in the 2nd row the dependence of the mean mass of the heavy fragment as a function of incident neutron energies. During the process of fitting the distributions we observed that the heavy fragment mass of the S2 fission mode only varies within 0.2 amu for all the studied neutron energies. So we have decided to fix this parameter in the fit to the

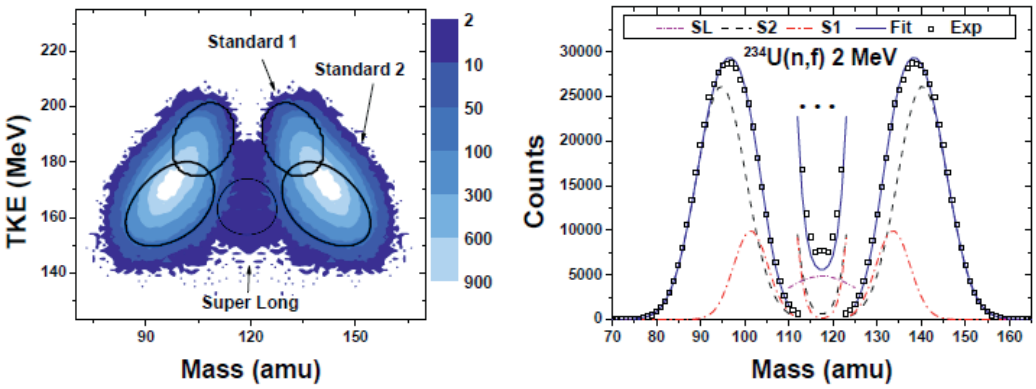

Fig. 11. Two-dimensional mass-TKE distribution (left part) with the indication of the fission modes by the full lines. Right part: The mass yield distribution for 2 MeV incident neutron energy on ^{234}U together with the contributions by the fission modes (S1, S2, SL, broken lines) and the total of the fit as full line.

value at 2 MeV incident neutron energy, which we have defined as the reference value. Doing so gives a clearer picture of the other parameters of the fit as a function of incident neutron energy, like for the dependence of the mean heavy fragment mass for the S1 mode. Here we see a clear drop of the mean value from about 134.2 amu at 0.2 MeV to about 133.6 amu at 2-2.5 MeV. Then the value for the mean heavy fragment mass stays more or less constant within 0.1 amu. This change in slope could hint to pair breaking in a similar way as observed in ^{238}U(n,f) [10]. The fission barrier is located at about 0.8 MeV, then the surplus excitation energy of the compound system when the sudden change in the mean heavy fragment mass for S1 happens is about 1.5 to 2 MeV. If we consider also the changes in the mean TKE (see Figure 10), where there is a definite drop in TKE around 2.5-3 MeV, then this supports the explanation that the behaviour in these two quantities of the fragments is due to pair breaking. Furthermore, a clear drop in the mean TKE of both the S1 and S2 mode is obvious (see 3rd row of Figure 12), except again around the vibrational resonance at E_n = 0.8 MeV. Finally, in the last row of Figure 12 the variance of the mass distributions for S1 and S2 is given. Here a drop in σ_m is discernible around 1 MeV and then in both cases a rise towards values as already observed at the lowest investigated incident neutron energies. A clear understanding of this phenomenon is still at stake.

Finally, Figure 13 shows the contribution of the changes in the mass and TKE distribution to the total changes in mean TKE as a function of incident neutron energy. The left part shows the changes in TKE due to changes in mass yield (TKEA) and changes in the TKE(A) distributions (TKETKE) for the experimentally measured distributions and the right part shows the same quantities for the fitted functions. There is a clear trend that the changes in the mean TKE are due mainly to the changes in the TKE(A) distributions (see Figure 9) and the changes in the mass yield distributions (see Figure 8) are not contributing much to the mean TKE, maybe except around the string vibrational resonance. This is confirmed by the fitted distributions as they follow the experimental ones rather closely. A similar behaviour was already observed in ^{235}U(n,f) [9]. In Ref. [10] for ^{238}U(n,f) a compensation effect was observed between the changes in the mass yield distribution and the changes in the TKE(A) distributions.

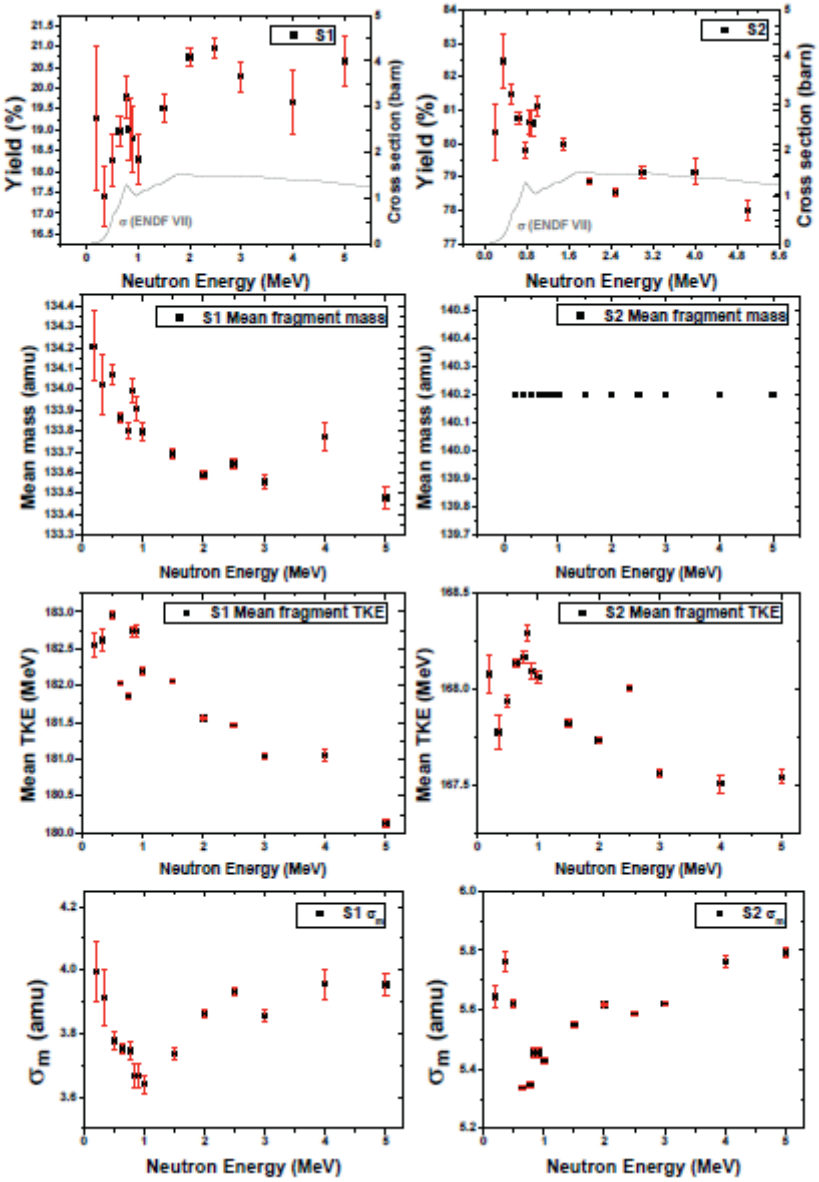

Fig. 12. Parameters of the fit for the S1 and S2 modes. Upper part Yields for the modes, next line: mean masses of the S1 and S2 modes, next line: mean TKE for S1 and S2 and lower part variance of the distributions.

4 Conclusions

The fission fragment mass and TKE distributions were measured for ^{234}U(n,f) from E_n = 0.2 MeV up to E_n = 5 MeV. The mean TKE as a function of incident neutron energy shows a peak around the vibrational resonance at about 0.8 MeV. This is in contradiction to results of Ref. [1], which showed a dip in the mean TKE at the resonance.

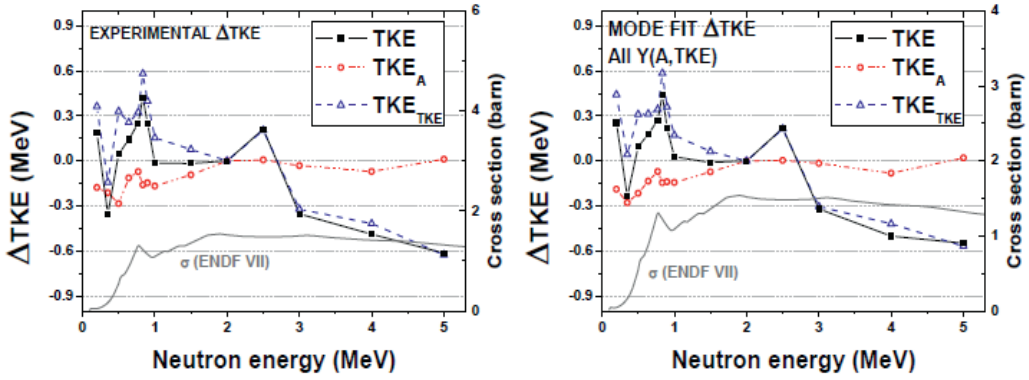

Fig. 13. Contribution of the changes in the mass and TKE distribution to the total changes in mean TKE as a function of incident neutron energy. The left part shows the changes in TKE due to changes in mass yield (TKE_A) and changes in the TKE(A) distributions (TKE_{TKE}) for the experimentally measured distributions and the right part shows the same quantities for the fitted functions.

Unfortunately not much is know about the experimental procedure and corrections applied in Ref. [1]. Both mass yield and TKE(A) distributions exhibit changes as a function of mass compared to the reference distributions at E_n = 2 MeV. The changes observed in mean TKE are mainly due to changes in the TKE(A) distributions as it was the case in ^{235}U(n,f) [9].

The angular distribution shows a strong anisotropy below 1 MeV with a peak close to the resonance, but at a bit higher incident neutron energy (see Figure 6) and a dip where the fission cross section shows some shoulder, the possible existence of a second resonance in the threshold of the fission cross section. This is in very good agreement with existing experimental data [5-7]. The mass and TKE distributions were analysed in terms of the multi-modal random-neck rupture model of Brosa et al. [11]. The yield of the standard 1 (S1) mode shows fluctuations in the threshold of the fission cross section due to the influence of the resonance and levels off at about 20% yield for higher incident neutron energies. The S2 mode shows the respective opposite behaviour. The mean TKE of both modes decreases with En. The decrease in mean TKE overrules the increase in S1 yield, so the mean TKE is dropping as a function of En above 2.5 MeV (see Figure 12).

References

1. A. Goverdovskii, Sov, Jour. Nucl. Phys **44**, 179 (1986)
2. E. Birgersson et al., Nucl. Phys. **A817**, 1 (2009)
3. http://www-nds.iaea.org/Th-U/ and related documents found on this webpage
4. A. Tudora, F.-J. Hambsch, Ann. Nucl. Phys. **37**, 771 (2010)
5. R. Lamphere, Nucl. Phys. **38**, 561 (1982)
6. A. Behkami et al., Phys. Rev. **171**, 1267 (1968)
7. J. Simmons and R. L. Henkel, Phys. Rev. **120**, 198 (1960)
8. A. Al-Adili et al., Nucl. Instr. Meth. **A624**, 684 (2010)
9. C. Straede et al., Nucl. Phys. **A462**, 85 (1987)
10. F. Vives et al., Nucl. Phys. **A662**, 63 (2000)
11. U. Brosa et al., Phys. Rep. **197**, 167 (1990)
12. ROOT program package, CERN